IJR International Journal of Railway
Vol. 3, No. 4 / December 2010, pp. 117-122

The Korean Society for Railway

Integration of Stress-Strain Rate Equations of CASM

Taehoon Koh†

Abstract

In transportation geotechnical engineering, stress-strain behavior of earth structures has been analyzed by numerical simulations with the implemented plasticity constitutive model. It is a fact that many advanced plasticity constitutive models on predicting the mechanical behavior of soils have been developed as well as experimental research works for geotechnical applications in the past decades. In this study, recently developed, a unified constitutive model for both clay and sand, which is referred to as CASM (clay and sand model), was compared with a classical constitutive model, Cam-Clay model. Moreover, integration methods of stress-strain rate equations using CASM were presented for simulation of undrained and drained triaxial compression tests. As a conclusion, it was observed that semi-implicit integration method has more improved accuracy of capturing strain rate response to applied stress than explicit integration by the multiple correction and iteration.

Keywords **:** *CASM (clay and sand model), Cam-Clay model, Semi-implicit integration, Explicit integration, Stress-strain rate equation*

1. Introduction

CASM was proposed by Yu (1998), and regarded as a simple, unified constitutive model based on critical-state theory. This model is able to predict the behavior of clay and sand more accurately, comparing with Cam-Clay model (Roscoe and Schofield, 1963) and Modified Cam-Clay model (Roscoe and Burland, 1968).

In this study, a unified constitutive model for both clay and sand, which is referred as CASM (clay and sand model), was compared with a classical constitutive model, Cam-Clay model. Moreover, integration methods of stress-strain rate equations using CASM were presented for simulation of undrained and drained triaxial compression tests.

2. CASM and Cam-Clay Model

2.1 Framework

Cam-Clay model can be derived from the virtual work theorem as:

$$dW_{ext}^{p} = p'd\varepsilon_{v}^{p} + qd\varepsilon_{s}^{p} = dW_{\text{int}}^{p} = Mp'd\varepsilon_{s}^{p} \quad (1)$$

where dW is the energy dissipated due to the plastic work, the external work done by the mean effective stress (p') and deviatoric stress (q) is equal to the internal work done by the shear stress, $d\varepsilon_{v}^{p}$ and $d\varepsilon_{s}^{p}$ are volumetric and shear plastic strain, respectively, and M is the ratio of q/p' at the critical state.

Then, flow rule and normality rule may be given as follows, respectively:

$$\frac{d\varepsilon_{v}^{p}}{d\varepsilon_{s}^{p}} = \left(d\lambda\frac{\partial g}{\partial p'}\right) \Big/ \left(\mathrm{d}\lambda\frac{\partial g}{\partial q}\right) = M - \eta \quad (2)$$

$$\left(\frac{dq}{dp'}\right) \times \left(\frac{d\varepsilon_{s}^{p}}{d\varepsilon_{v}^{p}}\right) = -1 \quad (3)$$

where η is the ratio of q/p' at yield.

Plastic potential (g) is able to be driven from Equations (2) and (3),

$$g = \left(\frac{\eta}{M}\right) + ln\left(\frac{p'}{p_{c}'}\right) \quad (4)$$

where p'_c indicates the size of the plastic potential.

In Cam-Clay model, the plastic potential(g) of Cam-Clay model is identical to the yield function (F).

† Corresponding author: Korea Railroad Research Institute
E-mail: thkoh@krri.re.kr

On the other hand, plastic potential of CASM follows Rowe's stress-dilatancy relation (Rowe, 1962) which defines the relationship between stress ratio and dilatancy rate:

$$\frac{d\varepsilon_v^p}{d\varepsilon_s^p} = \left(d\lambda\frac{\partial g}{\partial p'}\right)\Big/\left(d\lambda\frac{\partial g}{\partial q}\right) = \frac{9(M-\eta)}{9+3M-2M\eta} \tag{5}$$

Rowe's stress-dilatancy relation may be integrated to give the following plastic potential:

$$g = 3M\ln\frac{p'}{\xi} + (3+2M)\ln\left(\frac{2q}{p'}+3\right)$$

$$-(3-M)\ln\left(3-\frac{q}{p'}\right) = 0 \tag{6}$$

where ξ is size parameter.

Since CASM adopted the non-associated flow rule, plastic potential (Equation (6)) is not identical to the yield surface (Equation (7)):

$$F = \left(\frac{\eta}{M}\right)^n + \frac{\ln\left(\frac{p'}{p_c'}\right)}{\ln r} \tag{7}$$

The yield function of CASM is a form of generalized Cam-Clay model because the yield function of Cam-Clay model is able to be specified from CASM yield function using $n=1$ and $r=e$.

Different shapes of the plastic potentials of Cam-Clay, Modified Cam-Clay and CASM are shown in Fig. 1. The shape of CASM's plastic potential is very similar to that of the original Cam-clay model.

CASM has the same 5 model parameters ($M, \Gamma, \lambda, \kappa, v$) with those used in Cam-clay model (Fig. 2). In addition, two more parameters are needed to interpret CASM, i.e. r and n. r is the spacing ratio to control the intersection position of critical-state line and yield function. n is the stress-state coefficient to specify the shape of yield function, and the typical value of n is 1 to 5.

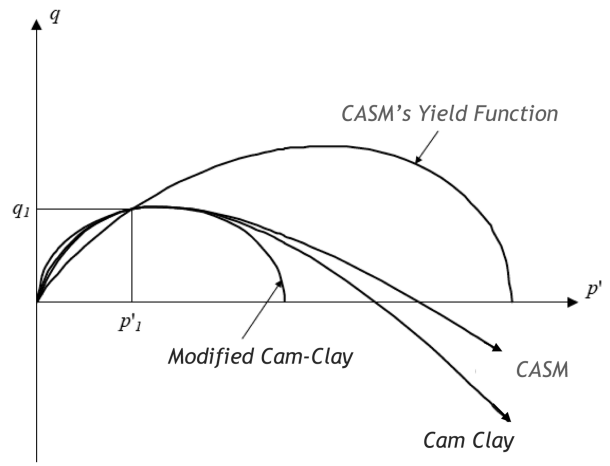

Fig. 1 Shapes of plastic potential surfaces (Modified after Khong, 2004)

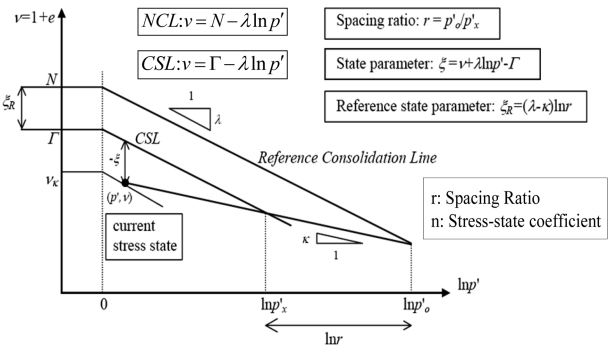

Fig. 2 Description of model parameters (Modified after Khong, 2004)

2.2 Limitations of Cam-Clay model

The original Cam-Clay model can capture the behavior of normally (NC) and lightly overconsolidated (OC) clay well. However, there are several limitations of these models as follows:

- Cam-Clay model does not take into account the anisotropy of soil which is one of the basic characteristics.
- Cam-Clay model cannot predict the stress-strain response of OC clay and that of sand (dilative soil).
- Cam-Clay model overestimates the failure stress on the dry side, etc.

3. Integration Methods

For the finite element analysis of elasto-plastic stress-strain behavior of soil in boundary-value problems, implementation of constitutive model in the finite element code requires a numerical integration of the constitutive stress-strain rate equations.

In this study, for integrating stress-strain rate equation, semi-implicit integration method is mainly used combining the simplicity of explicit method with the improved accuracy of implicit method.

In order to have the improved accuracy in semi-implicit method, the corrector is used during iteration in order to control the size of yield function.

The equations used for integration are given as follows:

Elastic moduli,

$$K = \frac{vp'}{\kappa}$$

$$G = \frac{3(1-2v)}{2(1+v)}K$$

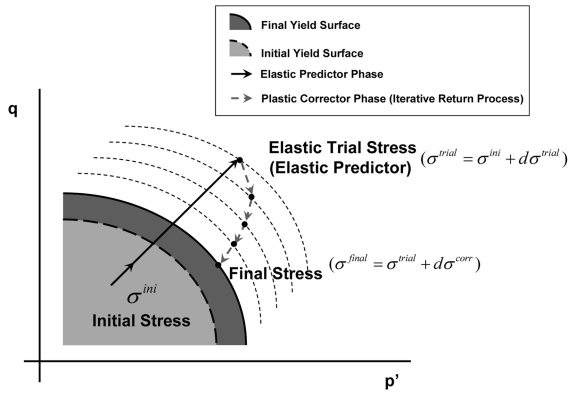

Fig. 3 Semi-implicit integration method (Modified after Ortiz and Simo, 1986)

Yield function,

$$F=\left(\frac{q}{Mp'}\right)^n+\frac{\ln\frac{p'}{p_c'}}{\ln\frac{p_c'}{p_x'}}$$

Plastic potential,

$$g=3M\ln\frac{p'}{\xi}+(3+2M)\ln\left(\frac{2q}{p'}+3\right)-(3-M)\ln\left(3-\frac{q}{p'}\right)$$

Hardening modulus,

$$H=\frac{v}{\xi_R}\left(\frac{9+6M}{2q+3p'}-\frac{9-3M}{3p'-q}\right)$$

where $\xi_R=(\lambda-\kappa)\ln\frac{p_c'}{p_x'}$

Differentiating F and g with respect to q and p',

$$\frac{\partial F}{\partial q}=n\left(\frac{q}{Mp'}\right)^{n-1}\frac{1}{Mp'}$$

$$\frac{\partial F}{\partial p'}=-n\left(\frac{q}{M}\right)^n\frac{1}{(p')^{n+1}}+\frac{1}{p'}\frac{1}{\ln\frac{p_c'}{p_x'}}$$

$$\frac{\partial g}{\partial q}=2\frac{3+2M}{2q+3p'}-\frac{3-M}{q-3p'}$$

$$\frac{\partial g}{\partial p'}=\frac{3M}{p'}-\frac{3+2M}{2q+3p'}\frac{2q}{p'}+\frac{3-M}{q-3p'}\frac{q}{p'}$$

3.1 Undrained Case

The flow chart for explicit and semi-implicit integration methods is shown in Fig. 4, which is under undrained triaxial compression condition.

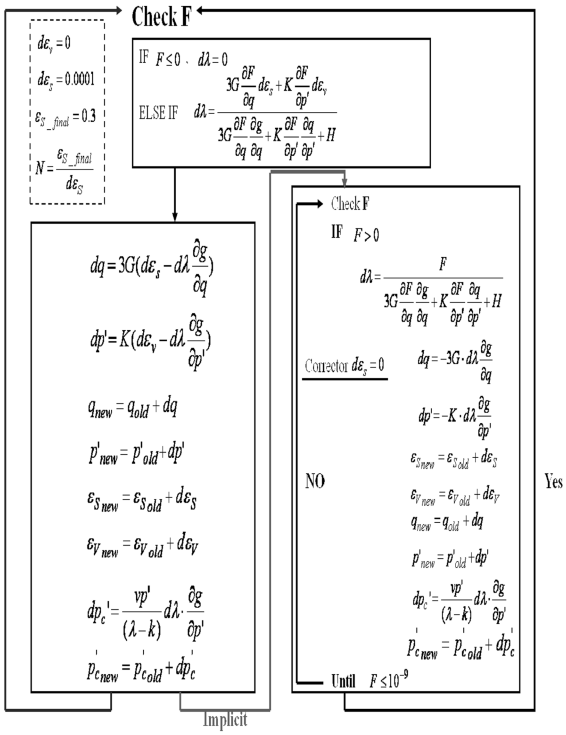

Fig. 4 Flow chart for integration methods under undrained triaxial compression condition

Variables for integration under undrained condition are as follows:

Linear elastic constitutive relationships are

$$\dot{q}=3G(\dot{\varepsilon}_s-\dot{\varepsilon}_s^p)$$

$$\dot{p}'=K(\dot{\varepsilon}_v-\dot{\varepsilon}_v^p) \tag{8}$$

Stress increment parameters are

$$\dot{q}=\dot{\sigma}_1-\dot{\sigma}_3$$

$$\dot{p}'=\frac{1}{3}(\dot{\sigma}_1+2\dot{\sigma}_3) \tag{9}$$

Strain increment parameters are

$$\dot{\varepsilon}_s=\frac{2}{3}(\dot{\varepsilon}_1-\dot{\varepsilon}_3)$$

$$\dot{\varepsilon}_v=\dot{\varepsilon}_1+2\dot{\varepsilon}_3 \tag{10}$$

By non-associated flow rule, plastic strain rates are

$$\dot{\varepsilon}_s^p=\dot{\lambda}\frac{\partial g}{\partial q}$$

$$\dot{\varepsilon}_v^p=\dot{\lambda}\frac{\partial g}{\partial p'} \tag{11}$$

Table 1 Unknown Values and Required Equations for Undrained Triaxial Compression Condition

Known Values	Unknown Values	Required Eqs.
$\dot{\varepsilon}_v = 0$	$\dot{q}$	(I)
$\dot{\varepsilon}_s = 0.0001$ $(\varepsilon_{s\_final} = 0.3)$	$\dot{p}'$	(II)
	$\dot{\lambda}$	(III)

Substituting Equation (10) into Equation (8),

$$\dot{q} = 3G\left(\dot{\varepsilon}_s - \dot{\lambda}\frac{\partial g}{\partial q}\right) \quad \text{(I)}$$

$$\dot{p}' = K\left(\dot{\varepsilon}_v - \dot{\lambda}\frac{\partial g}{\partial p'}\right) \quad \text{(II)}$$

where $\dot{\varepsilon}_v = 0$ since the volume is not changed through the test.

Procedures for estimation of Equation (III) and unknown value ($\dot{\lambda}$) are as follows:

From consistency condition ($\dot{F} = 0$),

$$\dot{F} = \frac{\partial F}{\partial q}\dot{q} + \frac{\partial F}{\partial p'}\dot{p}' - \dot{\lambda}\cdot H = 0 \quad \text{(III)}$$

Substituting Equations (I) and (II) into Equation (III),

$$\frac{\partial F}{\partial q}\left(3G\left(\dot{\varepsilon}_s - \dot{\lambda}\frac{\partial g}{\partial q}\right)\right) + \frac{\partial F}{\partial p'}\left(K\left(\varepsilon_v - \dot{\lambda}\frac{\partial g}{\partial p'}\right)\right) - \dot{\lambda}\cdot H = 0 \quad (12)$$

$$\dot{\lambda} = \frac{3G\frac{\partial F}{\partial q}\dot{\varepsilon}_s + K\frac{\partial F}{\partial p'}\dot{\varepsilon}_v}{3G\frac{\partial F}{\partial q}\frac{\partial g}{\partial q} + K\frac{\partial F}{\partial p'}\frac{\partial q}{\partial p'} + H}$$

3.2 Drained Case

The flow chart for explicit and semi-implicit integration methods is shown in Fig. 5, which is under drained triaxial compression condition.

Variables for integration under drained condition are as follows:

Linear elastic constitutive relationships are

$$\dot{q} = 3G(\dot{\varepsilon}_s - \dot{\varepsilon}_s^p)$$

$$\dot{p}' = K(\dot{\varepsilon}_v - \dot{\varepsilon}_v^p) \quad (13)$$

Stress increment parameters are

$$\dot{q} = \dot{\sigma}_1 - \dot{\sigma}_3$$

$$\dot{p}' = \frac{1}{3}(\dot{\sigma}_1 + 2\dot{\sigma}_3) \quad (14)$$

Strain increment parameters are

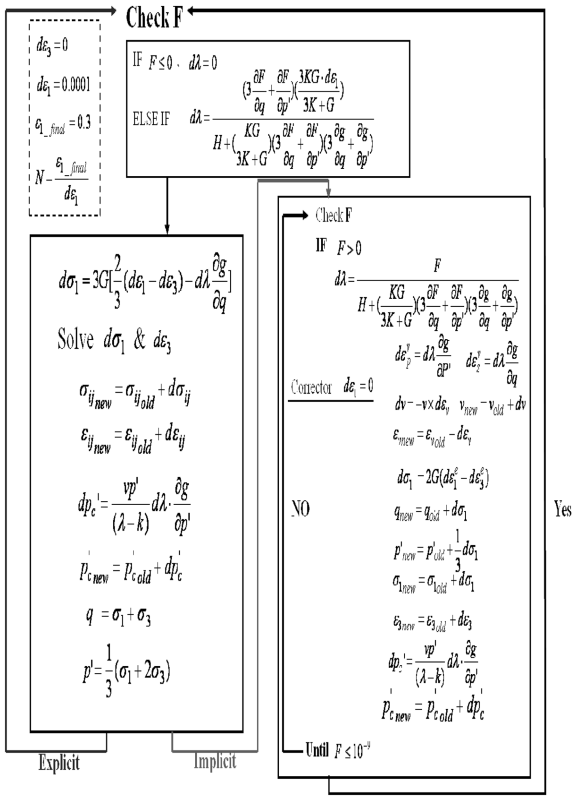

Fig. 5 Flow chart for integration methods under drained triaxial compression condition

$$\dot{\varepsilon}_s = \frac{2}{3}(\dot{\varepsilon}_1 - \dot{\varepsilon}_3)$$

$$\dot{\varepsilon}_v = \dot{\varepsilon}_1 + 2\dot{\varepsilon}_3 \quad (15)$$

By non-associated flow rule, plastic strain rates are

$$\dot{\varepsilon}_s^p = \dot{\lambda}\frac{\partial g}{\partial q}$$

$$\dot{\varepsilon}_v^p = \dot{\lambda}\frac{\partial g}{\partial p'} \quad (16)$$

Set Equation (13) is equal to Equation (14) after substituting Equations (15) and Equation (16) into Equation (13).

$$\dot{\sigma}_1 - \dot{\sigma}_3 = 3G\left(\frac{2}{3}(\dot{\varepsilon}_1 - \dot{\varepsilon}_3) - \dot{\lambda}\frac{\partial g}{\partial q}\right) \quad \text{(IV)}$$

$$\frac{1}{3}(\dot{\sigma}_1 + 2\dot{\sigma}_3) = K\left(\dot{\varepsilon}_1 + 2\dot{\varepsilon}_3 - \dot{\lambda}\frac{\partial g}{\partial p'}\right) \quad \text{(V)}$$

where $\dot{\sigma}_3 = 0$ since the confining stress is constant through the test.

Procedures for estimation of Equation (VI) and unknown

Table 2. Unknown Values and Required Equations for Drained Triaxial Compression Condition

Known Values	Unknown Values	Required Eqs.
$\dot{\sigma}_3 = 0$	$\dot{\sigma}_1$	(IV)
$\dot{\varepsilon}_1 = 0.0001$	$\dot{\varepsilon}_3$	(V)
	$\dot{\lambda}$	(VI)

values ($\dot{\sigma}_1, \dot{\varepsilon}_3, \dot{\lambda}$) are as follows:

From consistency condition ($F = 0$),

$$\dot{F} = \frac{\partial F}{\partial q}\dot{q} + \frac{\partial F}{\partial p'}\dot{p}' - \dot{\lambda} \cdot H = 0 \tag{17}$$

Substituting Equation (14) into Equation (17),

$$\frac{\partial F}{\partial q}(\dot{\sigma}_1 - \dot{\sigma}_3) + \frac{\partial F}{\partial p'}\left(\frac{1}{3}(\dot{\sigma}_1 + 2\dot{\sigma}_3)\right) - \dot{\lambda} \cdot H = 0$$

$$\frac{\partial F}{\partial q}\dot{\sigma}_1 + \frac{\partial F}{\partial p'}\left(\frac{1}{3}\dot{\sigma}_1\right) - \dot{\lambda} \cdot H = 0 \tag{VI}$$

From Equations (IV) and (V),

$$\dot{\sigma}_1 = 2G(\dot{\varepsilon}_1 - \dot{\varepsilon}_3) 3G\dot{\lambda}\frac{\partial g}{\partial q} \tag{18-a}$$

$$\dot{\sigma}_1 = 3K(\dot{\varepsilon}_1 + 2\dot{\varepsilon}_3) - 3K\dot{\lambda}\frac{\partial g}{\partial p'} \tag{18-b}$$

$$3K \cdot \dot{\sigma}_1 = 6KG\dot{\varepsilon}_1 - 6KG \cdot \dot{\varepsilon}_3 - 9KG\dot{\lambda}\frac{\partial g}{\partial q} \tag{19-a}$$

$$G \cdot \dot{\sigma}_1 = 3GK\dot{\varepsilon}_1 + 6GK\dot{\varepsilon}_3 - 3GK\dot{\lambda}\frac{\partial g}{\partial p'} \tag{19-b}$$

$\dot{\sigma}_1$ can be determined from the summation of Equations (19-a) and (19-b) as follows:

$$(3K+G) \cdot \dot{\sigma}_1 = 9KG\dot{\varepsilon}_1 - 3KG\dot{\lambda}\left(3\frac{\partial g}{\partial q} + \frac{\partial g}{\partial p'}\right)$$

$$\dot{\sigma}_1 = \frac{9KG\dot{\varepsilon}_1 - 3KG\dot{\lambda}\left(3\frac{\partial g}{\partial q} + \frac{\partial g}{\partial p'}\right)}{(3K+G)} \tag{20}$$

$\dot{\lambda}$ can be determined from substituting Equation (20) into Equation (VI).

$$\left(\frac{\partial F}{\partial q} + \frac{1}{3}\frac{\partial F}{\partial p'}\right)\frac{9KG\dot{\varepsilon}_1 - 3KG \cdot \dot{\lambda}\left(3\frac{\partial g}{\partial q} + \frac{\partial g}{\partial p'}\right)}{(3K+G)} - \dot{\lambda} \cdot H = 0$$

$$\left(\frac{\partial F}{\partial q} + \frac{1}{3}\frac{\partial F}{\partial p'}\right)\left(9KG\dot{\varepsilon}_1 - 3KG \cdot \dot{\lambda}\left(3\frac{\partial g}{\partial q} + \frac{\partial g}{\partial p'}\right)\right)$$

$$-\dot{\lambda} \cdot H(3K+G) = 0$$

$$\dot{\lambda} = \frac{\left(\frac{\partial F}{\partial q} + \frac{1}{3}\frac{\partial F}{\partial p'}\right)(9KG\dot{\varepsilon}_1)}{H(3K+G) + 3KG\left(\frac{\partial F}{\partial q} + \frac{1}{3}\frac{\partial F}{\partial p'}\right)\left(3\frac{\partial g}{\partial q} + \frac{\partial g}{\partial p'}\right)} \tag{21}$$

$\dot{\varepsilon}_3$ can be determined from Equation (18-a).

$$\dot{\varepsilon}_3 = \frac{2G\dot{\varepsilon}_1 - \dot{\sigma}_1 - 3G\dot{\lambda}\frac{\partial g}{\partial q}}{2G}$$

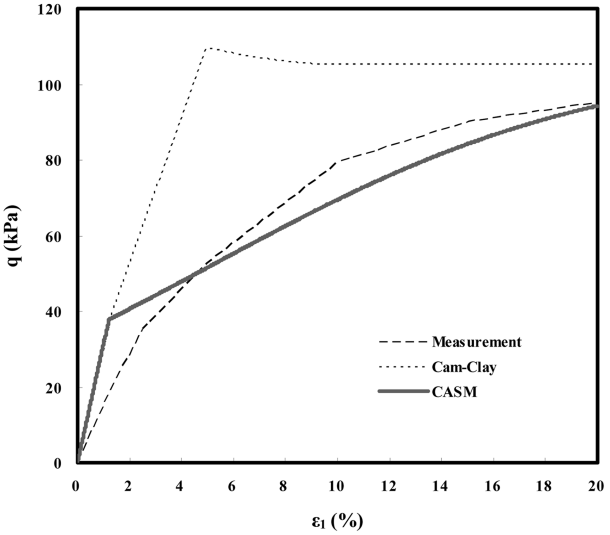

(a) Undrained loading

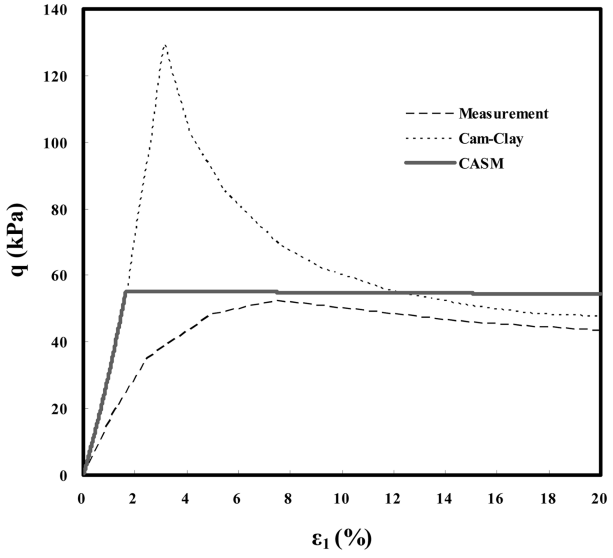

(b) Drained loading

Fig. 6 Comparison of stress-strain response for heavily overconsolidated Weald clay

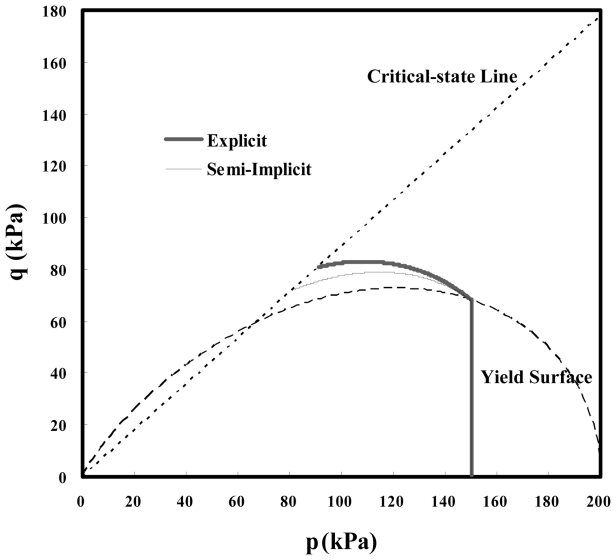

Fig. 7 Comparison of integration methods for London clay under undrained triaxial compression condition

4. Simulations

Fig. 6 shows the simulations of the triaxial compression tests for heavily overconsolidated Weald clay (OCR=24) using the constitutive models. The stress-strain response was predicted by implementation of Cam-Clay model (model parameters; M=0.9, Γ =2.06, λ =0.093, κ =0.025, υ = 0.3, r=2.718, n=1.0) and CASM (model parameters; M=0.9, Γ =2.06, λ =0.093, κ =0.025, υ =0.3, ξ =0.0679, n=4.5), and compared to the test results under undrained and drained triaxial compression conditions.

It was shown that CASM broadly simulated well the undrained test (Fig. 6 (a)). As shown in Fig. 6 (b), although the predicted axial strains for the shear strength (peak deviatoric stress) were smaller than those observed in tests, in general, CASM captured well the stress-strain response in the pre-peak and post-peak regimes. However, Cam-Clay model showed the limitation to predict the behavior of OC clay.

Fig. 7 shows the results from explicit and semi-implicit integration procedures for London clay (OCR=2-4) under undrained triaxial compression condition in which CASM parameters are M=0.888, Γ =2.759, λ =0.161, κ =0.062, υ =0.3, r=3.0, and n=2.0.

At 150 kPa confining stress, the predicted response by the semi-implicit integration was more accurate to the experimental results than that by explicit method.

5. Conclusion

In this study, a unified constitutive model, CASM (clay and sand model), was compared with a classical constitutive model, Cam-Clay model. It can be concluded that based on the good agreement between the simulations and the experimental results, the framework of CASM is useful for modeling the undrained and drained response of soil.

Moreover, explicit and semi-implicit integration methods of stress-strain rate equations were presented for simulation of undrained and drained triaxial compression loading. In comparing the predicted and experimental responses, it can be seen that the semi-implicit integration method captured well the main features of soil behavior because of the improved accuracy in semi-implicit method.

Reference

1. Khong, C.D. (2004). "Development and numerical evaluation of unified critical state models," Ph. D. Thesis, University of Nottingham.
2. Ortiz, M. and Simo, J.C. (1986). "An analysis of a new class of integration algorithms for elasto-plastic constitutive relations," International Journal for Numerical Methods in Engineering, Vol. 23, No. 3, pp. 353-366.
3. Roscoe, K.H. and Burland, J.B. (1968). "On the generalized stress strain behaviour of wet clay," Engineering Plasticity, Cambridge University Press, pp. 535-609.
4. Roscoe, K.H. and Schofield, A.N. (1963). "Mechanical behaviour of an idealized wet clay," Proceedings of the 2nd European Conference on Soil Mechanics and Foundation Engineering (ECSMFE), Vol. 1, pp. 47-54.
5. Rowe, P.W. (1962). "The stress-dilatancy relation for static equilibrium of an assembly of particles in contact," Proceedings of the Royal Society of London, Series A, Mathematical and Physical Sciences, Vol. 269, No. 1339, pp. 500-527.
6. Yu, H.S. (1998). "CASM: a unified state parameter model for clay and sand," International Journal for Numerical and Analytical Methods in Geomechanics, Vol. 22, No. 8, pp. 621-653.